Rotor Position Estimation Method of Sensorless PM Motor at Rest with No Sensitivity to Armature Resistance

Toshihiko Noguchi, Kazunori Yamada, Seiji Kondo and Isao Takahashi
Nagaoka University of Technology
1603-1 Kamitomioka, Nagaoka, Niigata 940-21 Japan

Abstract – **A new rotor position estimation method of a sensorless PM motor at rest is proposed, which has no sensitivity to the armature resistance. The method is based on a saliency of the rotor, and utilizes the alternating magnetic field which is excited by current control. The phase difference between the magnetizing current and the voltage references makes it possible to estimate the rotor direction accurately without motor parameters except the ratio of *d*-axis and *q*-axis inductances. In addition, the magnetic pole can be identified evidently using the voltage reference vibration phenomena caused by magnetic saturation.**

I. INTRODUCTION

PM motors with salient magnetic poles have been employed as high performance servo actuators in FA components, and many papers have reported their applications for electrical vehicles in recent years. The output torque of the PM motor is controlled by its armature currents according to the rotor position; hence a sensor mounted on the rotor shaft is necessary to detect the rotor position. It is desired strongly to remove the position sensor, which has several problems concerning reliability and implementation. In order to attain sensorless operation, estimation of the rotor position is essential not only at running state but also at stationary state. Therefore, several estimation methods at rest were proposed, which were based on a pilot voltage signal[1][2], current vector locus[3] and so on. The former method seems to be difficult to detect the current peak values accurately. The latter method requires precise control of the applied armature voltage.

This paper proposes a new rotor position estimation method of the PM motor at rest, which has no sensitivity to the armature resistance. The method has the advantage of robustness against the cable resistance between the controller and the motor, which is not negligible for such applications as deep underground well pump drives. In addition, when the motor is implemented on the electrical vehicles, the method can estimate the rotor position accurately with no dependence on the motor temperature. The method is based on a saliency of the rotor, and applies the alternating magnetic field to the motor which is excited by current control. In what follows, theoretical consideration is developed, and several simulation and experimental results are presented.

II. ROTOR POSITION ESTIMATION METHOD

A. Estimation of Rotor Direction

Fig. 1 shows a relation between the rotor position of the PM motor and the coordinates: α-β and d-q coordinates are defined as stator and rotor reference frames respectively. As shown in Fig. 2, the alternating magnetic field is applied to the motor by current control, and the frequency of the current reference is so high as not to rotate the motor. Then two kinds of phase differences between the currents and the voltages are detected, which make it possible to estimate the rotor position independently of the armature resistance.

First of all, the estimated rotor direction is set to zero temporarily, that is $\hat{\theta}=0$, to excite the motor in the direction of the α-axis, not the d-axis nor the q-axis, and the following current is applied to the motor:

$$\begin{bmatrix} i_\alpha \\ i_\beta \end{bmatrix} = \begin{bmatrix} I_1 \cos \omega t \\ 0 \end{bmatrix}. \tag{1}$$

The motor parameters and variables are defined as follows:

v_α and v_β : α and β-axis voltages,

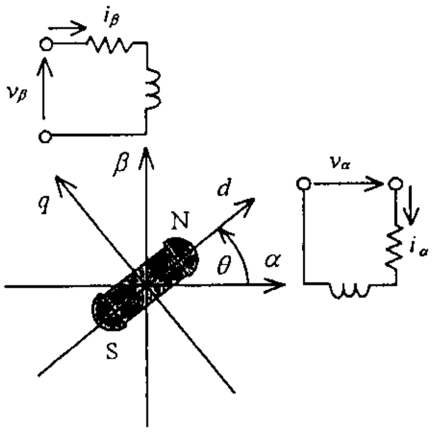

Fig. 1. Relation between rotor position and coordinates.

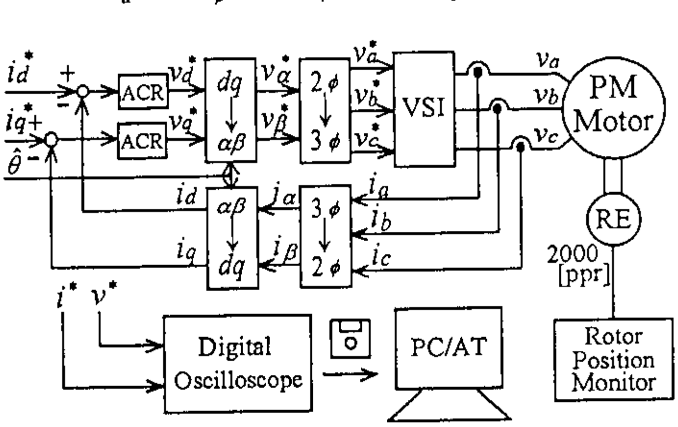

Fig. 2. Configuration of experimental system.

i_α and i_β : α and β-axis currents,
ω : operating angular frequency,
R_a : armature resistance,
L_d : d-axis inductance,
L_q : q-axis inductance.

The current amplitude I_1 is set at the small value which does not cause magnetic saturation. Then the following voltages are observed in the corresponding windings:

$$\begin{bmatrix} v_\alpha \\ v_\beta \end{bmatrix} = \begin{bmatrix} R_a I_1 \cos\omega t - \omega\left(L_d \cos^2\theta + L_q \sin^2\theta\right) I_1 \sin\omega t \\ \omega \sin\theta \cos\theta \left(L_q - L_d\right) I_1 \sin\omega t \end{bmatrix}. \quad (2)$$

The phase difference φ_α between i_α and v_α is derived from (1) and (2) as

$$\tan\varphi_\alpha = \frac{\omega\left(L_d \cos^2\theta + L_q \sin^2\theta\right)}{R_a}. \quad (3)$$

Equation (3) shows that the φ_α is a function of the rotor position θ because of the saliency of the rotor, that is $L_d \neq L_q$. It is possible to estimate θ by using this equation, however the all of the motor parameters are necessary to calculate the equation. In order to solve the problem, the motor is also excited in the direction of the β-axis, and the following current is applied to the motor in a similar way:

$$\begin{bmatrix} i_\alpha \\ i_\beta \end{bmatrix} = \begin{bmatrix} 0 \\ I_1 \cos\omega t \end{bmatrix}. \quad (4)$$

This results in the following voltages:

$$\begin{bmatrix} v_\alpha \\ v_\beta \end{bmatrix} = \begin{bmatrix} \omega \sin\theta \cos\theta \left(L_q - L_d\right) I_1 \sin\omega t \\ R_a I_1 \cos\omega t - \omega\left(L_d \sin^2\theta + L_q \cos^2\theta\right) I_1 \sin\omega t \end{bmatrix}. \quad (5)$$

In this case, the phase difference φ_β between i_β and v_β is derived from (4) and (5) as

$$\tan\varphi_\beta = \frac{\omega\left(L_d \sin^2\theta + L_q \cos^2\theta\right)}{R_a}. \quad (6)$$

The phase differences in (3) and (6) are different. Solving (3) and (6) with respect to θ as a pair of simultaneous equations and eliminating R_a, the estimated rotor position $\hat{\theta}$ is derived as

$$\hat{\theta} = \pm\tan^{-1}\sqrt{\frac{k_L \tan\varphi_\alpha - \tan\varphi_\beta}{k_L \tan\varphi_\beta - \tan\varphi_\alpha}}, \quad (7)$$

where $k_L = L_q / L_d$. It is found that (7) does not need any absolute motor parameters except the inductance ratio k_L. It is not possible to keep high precision when $\hat{\theta}$ is nearly equal to $\pi/2$, therefore, $\hat{\theta}$ is estimated actually by the following equations:

$$\hat{\theta} = \pm\tan^{-1}\sqrt{\frac{A}{B}} \qquad (\text{if } A \leqq B), \quad (7a)$$

$$\hat{\theta} = \frac{\pi}{2} \pm \tan^{-1}\sqrt{\frac{B}{A}} \qquad (\text{if } A > B), \quad (7b)$$

where $A = k_L \tan\varphi_\alpha - \tan\varphi_\beta$, and $B = k_L \tan\varphi_\beta - \tan\varphi_\alpha$.

The estimated rotor position $\hat{\theta}$ is not possible to be determined uniquely, however, because of a double sign in (7). Therefore, the voltage equation of which current is controlled to be zero is used to determine the sign of (7). For example, the second low of (2) is modified as

$$\sin\theta\cos\theta = \frac{v_\beta}{\omega\left(L_q - L_d\right) I_1 \sin\omega t}. \quad (8)$$

When the right hand of (8) is positive, the rotor position exists in the first or the third quadrant. When it is negative, the position exists in the second or the fourth quadrant. Therefore, the rotor direction is determined uniquely without the value of the motor parameters. Procedure of the rotor direction estimation is summarized in Fig. 3 (a).

B. Identification of Magnetic Pole

The rotor direction is estimated uniquely by (7) and (8), but it is not apparent whether the estimated direction corresponds to N pole or S pole of the rotor magnet. In what follows, the identification technique by using the voltage reference vibration phenomena caused by the magnetic saturation is described. The rotor direction $\hat{\theta}$ estimated by (7) and (8) is applied in the current control loop shown in Fig. 2. Then the following d-axis current is applied to the motor:

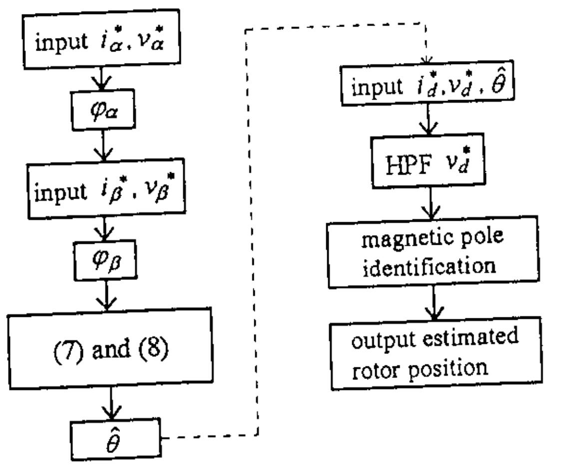

(a) Rotor direction estimation. (b) Magnetic pole identification.
Fig. 3. Procedures of rotor position estimation.

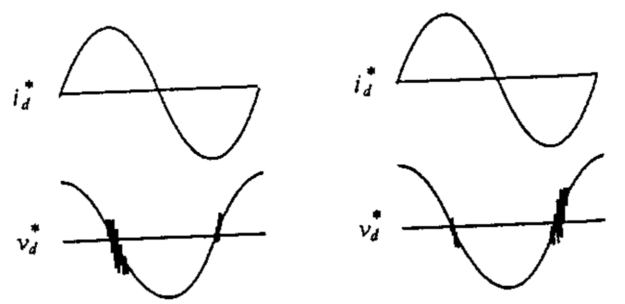

(a) d-axis conforms to N pole. (b) d-axis conforms to S pole.
Fig. 4. Illustration of voltage and current waveforms in magnetic saturation region.

$$\begin{bmatrix} i_d \\ i_q \end{bmatrix} = \begin{bmatrix} I_2 \cos\omega t \\ 0 \end{bmatrix}, \quad (9)$$

where the amplitude I_2 is set at the value which can bring the magnetic saturation in the motor. Consequently, owing to the magnetic saturation, the vibration phenomena of the voltage reference are observed near the current peaks as illustrated in Fig. 4. The phase relation between the phenomena and the current is found to be different depending on the magnet polarity as shown in Fig. 4. The proposed method utilizes the phenomena mentioned above, and also enables to identify the magnetic pole of the rotor with no parameter sensitivities. Fig. 3 (b) summarizes the Procedure of magnetic pole identification.

III. Simulation Results

A. System Configuration

Several simulations were conducted to examine the estimation characteristics of the rotor position. TABLE I shows the rated values and the nominal parameters of the tested motor. Current control loops are adopted as shown in Fig. 2, and the inverter is assumed to have no forward drops in the switching devices and no dead time. The PWM method is based on a standard subharmonic carrier modulation of which frequency is 15 kHz.

B. Simulation Results of Rotor Direction Estimation

The rotor position $\hat{\theta}$ is set at zero temporarily to excite the motor in the direction of the α or β-axis, and the current shown in (1) or (4) is applied to the motor. In the simulation, the magnetic saturation characteristics are assumed to be a combination of several polynomial functions. The current

TABLE I Rated Values and Nominal Parameters of Tested Motor

rated power	100 (W)	L_d	184.4 (mH)
rated speed	1500 (rpm)	L_q	276.6 (mH)
rated current	0.7 (A)	Ψ	0.306 (Wb)
number of poles	4 (pole)	J_m	0.004143 (kgm^2)
R_a	14.69 (Ω)	D_r	0.0001 (Nms/rad)

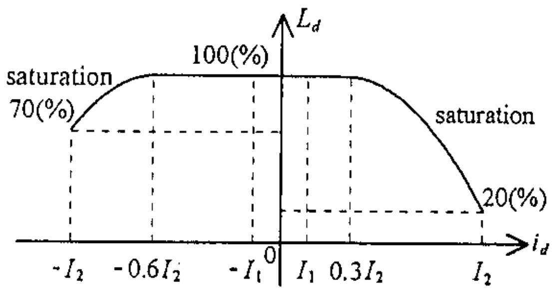

Fig. 5. Assumed inductance characteristics.

amplitude I_1 is set at so small value as not to bring the magnetic saturation as shown in Fig. 5. The exciting current frequency was 50 Hz. Fig. 6 shows the simulation results under the condition of θ = 30 deg (mechanical degree) (a true value of the rotor position) and nominal R_a. The phase differences φ_α from Fig. 6 (a) and φ_β from Fig. 6 (b) are

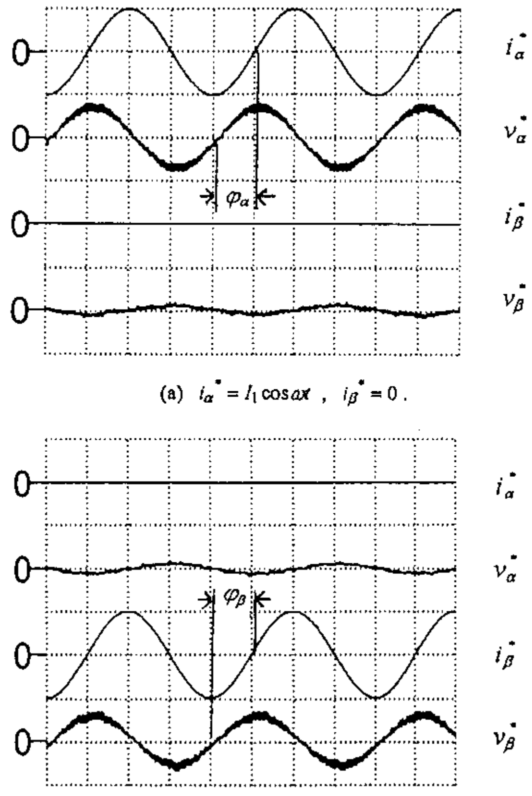

(b) $i_\alpha^* = 0$, $i_\beta^* = I_1 \cos\omega t$.
i : 0.17(A/div) , v : 19.2(V/div) , t : 5(ms/div)
Fig. 6. Voltage and current waveforms on rotor direction estimation (simulation results).

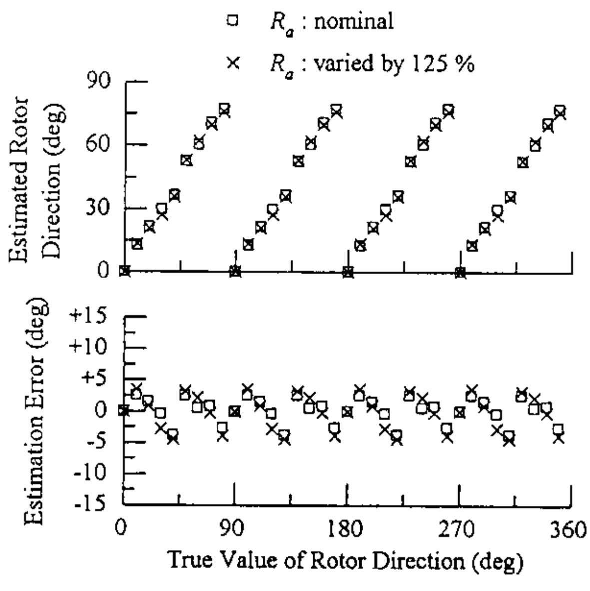

Fig. 7. Results of rotor direction estimation(simulation results).

measured by using the current references and the voltage references. The measured φ_α and φ_β is substituted into (7), and a sign of (7) is determined by (8) to estimate the rotor direction uniquely. Fig. 7 shows the estimation results all over the range of 0 to 360 deg (mechanical degree), and also shows the results under the condition of varied R_a by 125 %. The estimation results of the rotor direction conform very well to the true values periodically even if R_a varies. The estimation error was within +3.5 to -4.2 deg (mechanical degree). The periodical characteristics of the estimated rotor direction imply that the polarity of the magnetic pole has to be identified, which is described in the next section.

Equation (7) requires the ratio k_L of d-axis and q-axis inductances; hence it is important to examine the effect of its parameter mismatch. Fig. 8 shows the simulation results of the estimation characteristics when the mismatch of k_L occurs. The simulations were carried out in the case that the parameter mismatch is only in L_q. From Fig. 8, it is found that the +25 % parameter mismatch does not affect so much, but -25 % parameter mismatch detrimentally affects the estimation error. Therefore, the exact adjustment of k_L is substantial for the accurate estimation of the rotor direction.

C. Simulation Results of Magnetic Pole Identification

The rotor direction $\hat{\theta}$ estimated by (7) and (8) is used in the current control loop shown in Fig. 2, and the current represented by (9) is applied to the motor. The inductance shows asymmetrical characteristics with respect to the current polarity because of the permanent magnet of the rotor as shown in Fig. 5. Fig. 9 shows the simulation results. Fig. 9 (a) corresponds to the case that the d-axis conforms to the N pole, while Fig. 9 (b) corresponds to the case that the d-axis conforms to the S pole. From these figures, it is found that the magnetic saturation causes vibrations of the voltage reference near the current peaks, and the phase relation between the current reference and the vibrations depends on weather the d-axis conforms to the N pole or the S pole. This vibration phenomena are possibly caused by a reaction of high gain current control. Since the high loop gain can magnify the indication of the magnetic saturation, the proposed method does not require high currents to identify the magnetic pole obviously. Fig. 10 shows the results over the range of 0 to 360 deg (mechanical degree). Vertical axis of the figure represents the ratio which is calculated from the vibration counts during the positive and negative current

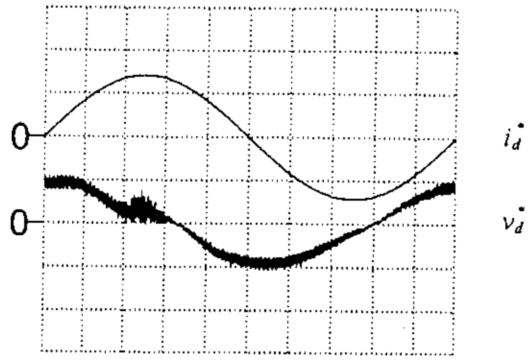

(a) d-axis conforms to N pole.

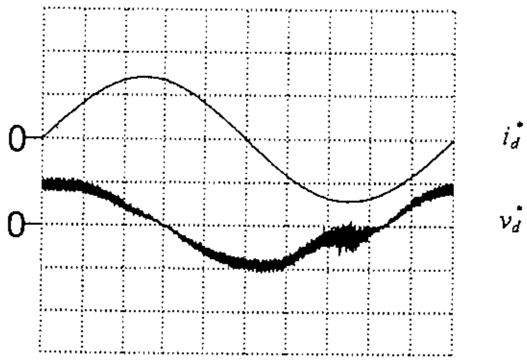

(b) d-axis conforms to S pole.
i : 0.85(A/div) , v : 76.8(V/div) , t : 2(ms/div)
Fig. 9. Voltage and current waveforms on magnetic pole identification (simulation results).

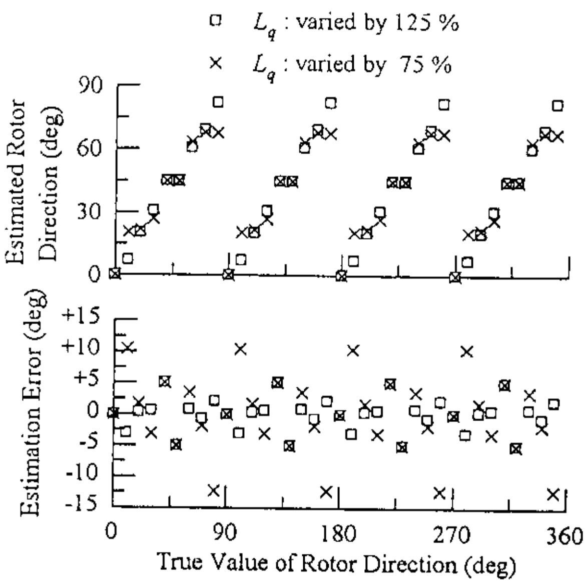

Fig. 8. Results of rotor direction estimation with varied L_q (simulation results).

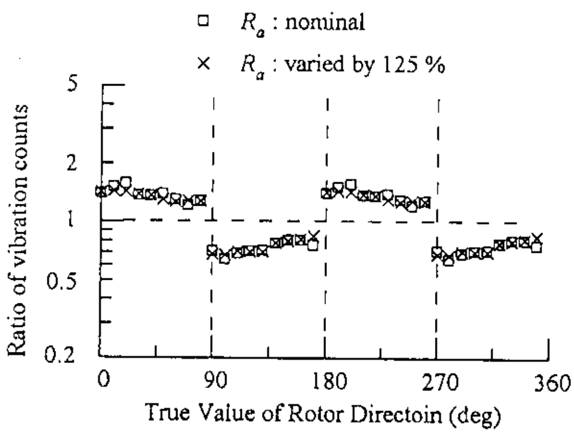

Fig. 10. Results of magnetic pole identification (simulation results).

periods. The number of vibrations can be counted by using a simple high pass filter and a hysteresis comparator. It is found that the ratio becomes greater than one when the d-axis conforms to the N pole, while the ratio becomes less than one when the d-axis conforms to the S pole.

IV. EXPERIMENTAL SYSTEM AND RESULTS

A. Configuration of Experimental System

Experimental system was constituted as shown in Fig. 2. The VSI is a voltage source inverter of which pulse width modulator is based on a subharmonic method, and its carrier frequency is 15 kHz. The VSI employs IGBT modules as power switching devices. Armature currents of the PM motor are detected by Hall-CTs, and are controlled by some analogue circuits. The true value of the rotor position is detected with a rotary encoder mounted on its shaft for monitoring. The current and voltage references are measured with a digitized oscilloscope, and the data are input to a host computer via floppy disks. In order to eliminate the PWM ripples and noises, a low pass filter (LPF) of 650 Hz cut off frequency is constituted by software. The phase difference between the current and voltage references through the above LPF is detected, and the estimated rotor direction is obtained by using (7) and (8). After the obtained result is applied to the coordinate transformation circuits, a current loop gain is increased to identify the magnetic pole. The fundamental frequency component of the voltage reference is eliminated by a high pass filter (HPF) of 2 kHz cut off frequency. The output of the HPF is used to count the number of times of the vibrations. Finally, The identification of the magnetic pole is done by evaluating the ratio of the vibration counts during the positive and negative current periods.

B. Experimental Results of Rotor Direction Estimation

An initial estimated rotor position is set at zero temporarily to excite the motor in the direction of α or β-axis. Fig. 11 shows examples for 30 deg (mechanical degree) of the true rotor position. Fig. 11 (a) corresponds to the condition of (1) and (2), while Fig. 11 (b) corresponds to the condition of (4) and (5). The phase differences φ_α and φ_β are detected from the data shown in Fig. 11, and the rotor direction is estimated by using (7) and (8). The experimental results of the estimation is shown in Fig. 12. In the figure, the estimated rotor directions are plotted against the true values all over the mechanical angle of 0 to 360 deg (mechanical degree). The experiments were conducted in the cases of nominal and varied armature resistances. When R_a was varied by 125 %, external resistances were added in series with the armature windings. As can be seen in the figure, the estimated rotor directions conform very well to the true values periodically, and the estimation error was within the range of +2.5 to -4.5 deg (mechanical degree). Since the error is so small, sensorless operation is possible from starting at rest without any reverse rotation or pull out phenomena. The estimation error of the experimental results is smaller than that of simulation results, because the averaging function of digitized oscilloscope was used to detect the current and voltage references to eliminate the PWM ripples. It was confirmed that the proposed method did

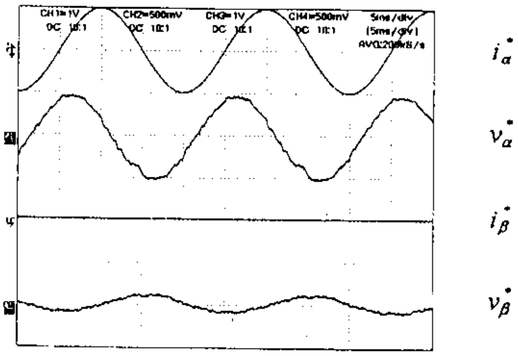

(a) $i_\alpha^* = I_1 \cos\omega t$, $i_\beta^* = 0$.

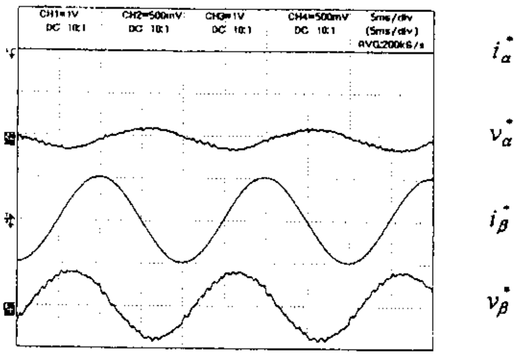

(b) $i_\alpha^* = 0$, $i_\beta^* = I_1 \cos\omega t$.
i : 0.17(A/div) , v : 19.2(V/div) , t : 5(ms/div)

Fig. 11. Voltage and current waveforms on rotor direction estimation (experimental results).

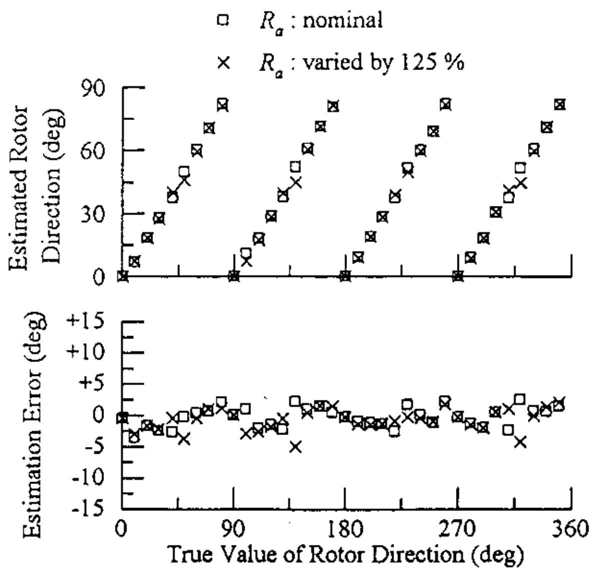

Fig. 12. Results of rotor direction estimation (experimental results).

not have sensitivity to the armature resistance variation. In addition, the method does not require any voltage sensors to detect the phase differences, because the reference values are used instead of the actual values.

C. Experimental Results of Magnetic Pole Identification

Fig. 13 shows the experimental results of magnetic pole identification. Fig. 13 (a) corresponds to the case that the N pole is in the direction of d-axis, while Fig. 13 (b) corresponds to the case that the S pole is in the direction of d-axis. The vibration phenomena of the voltage references are observed near the current peaks as described before. In these figures, it is found that the number of vibrations is less than that of the simulation result. However, the phenomena always appear in the same phase, and depend on weather the d-axis conforms to the N pole or the S pole.

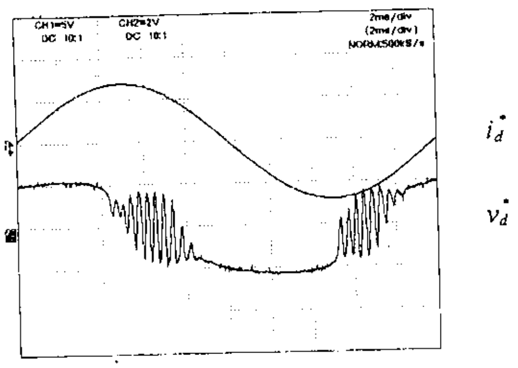

(a) d-axis conforms to N pole.

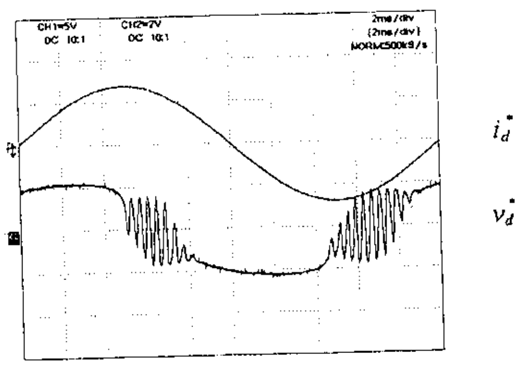

(b) d-axis conforms to S pole.
i : 0.85(A/div) , v : 76.8(V/div) , t : 2(ms/div)
Fig. 13. Voltage and current waveforms on magnetic pole identification (experimental results).

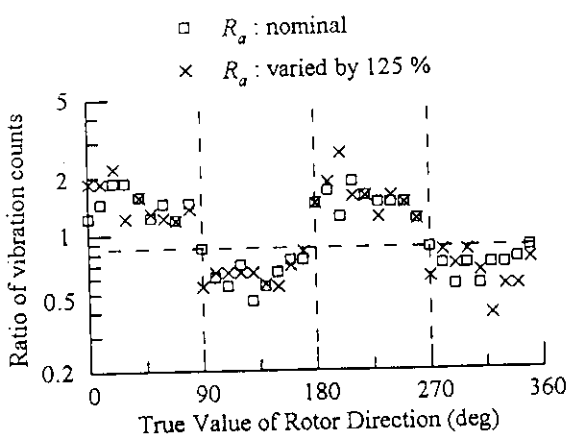

Fig. 14. Results of magnetic pole identification (experimental results).

Fig. 14 shows the experimental results over the range of 0 to 360 deg (mechanical degree). In the figure, the ratio of vibration counts is plotted against the true rotor position. When the N pole is in the direction of assumed d-axis, the ratio is greater than one. On the other hand, when the S pole is in the direction of assumed d-axis, the ratio becomes less than one. The ratio was within the range of 0.5 to 2.0 in the experiment. Since the ratio is distributed separately from one, the magnetic pole is possible to be identified evidently. The results also show that the proposed method is not sensitive to the variation of R_a.

V. CONCLUSION

In this paper, a new rotor position estimation method of a sensorless PM motor at rest has been proposed, which has no sensitivity to the armature resistance. The method is based on a saliency of the rotor, and utilizes the alternating magnetic field which is excited by current control. The rotor direction can be estimated accurately by using phase differences between the magnetizing currents and the voltage references without any motor parameters except the ratio of d-axis and q-axis inductances. In addition, the magnetic pole can be identified evidently by using voltage reference vibration phenomena caused by the magnetic saturation. The simulation and the experiment were conducted on the basis of the above theoretical analysis, and it was confirmed that the rotor position could be estimated with the error within +2.5 to -4.5 deg (mechanical degree) even if the armature resistance varied up to 125 % of the nominal value.

REFERENCES

[1] M. Naidu and B. K. Bose, "Rotor Position Estimation Scheme of a Permanent Magnet Synchronous Machine for High Performance Variable Speed Drive," *IEEE IAS Annual Meeting Conference Records*, pp. 48-53, 1992.

[2] N. Matsui and T. Takeshita, "A Novel Starting Method of Sensorless Salient-Pole Brushless Motor," *IEEE IAS Annual Meeting Conference Records*, pp. 386-392, 1994.

[3] S. Kondo, A. Takahashi and T. Nishida, "Armature Current Locus Based Estimation Method of Rotor Position of Permanent Magnet Synchronous Motor without Mechanical Sensor," *IEEE IAS Annual Meeting Conference Records*, pp. 55-60, 1995.